MAGNET TECHNOLOGY

Void Fraction Effect on AC Loss in Saturation Regime for NbTi CIC Conductor

Baudouy, B., NHMFL
Berenguer, C., INSA-Toulouse
Van Sciver, S.W., NHMFL/FAMU-FSU College of Engineering

The NHMFL TACL Facility was used to perform AC loss measurements on NbTi Cable-In-Conduit Conductor (CICC) samples.[1] AC loss tests have been performed over a range of field variation rates, high enough that the saturation regime is obtained. From these measurements, the effective coupling current time constants and the effective radius of the saturated cable stage are determined. The losses have been modeled in a saturated regime using an extrapolated model for a monolithic conductor (Figure 1).[2] As expected, AC losses increase as the void fraction decreases. The effective time constant and the "saturated" radius increase with decreasing void fraction (Table 1). The determination of these radii shows that the predominant coupling current losses are not located in the last sub-cable, but rather at an intermediate sub-cable. This effect has already been revealed in our previous study[3]. It can be explained by the fact that the strands are submitted to higher stresses in intermediate stages. It is of a great interest for CICC designers because it shows that wrapping stainless steel foil around

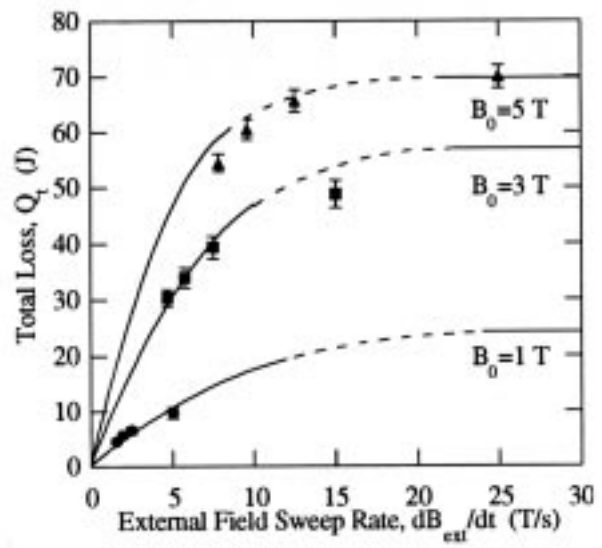

Figure. 1. AC loss measurements and fitted curves for 40% void fraction sample versus external field sweep rate (B_0=1T, ■ B_0=3T and ▲ B_0=5T).

Table 1. Time Constant

Conductor's Void Fraction	40%	45%	50%
τ (ms)	45±3	30±3	30±3

the last sub-cable may not reduce the coupling current losses.

References:

1 Baudouy, B., *et al.*, "Void Fraction Effect on AC Loss in Saturation Regime for NbTi CIC Conductor," presented at ASC '98, September 1998.
2 Ciazynski, D., *et al.*, Cryogenics, 22, 507 (1984).
3 Bonito Oliva, A., *et al.*, IEEE Trans. Magn., 32, 4, 2834 (1996).

Comparison of the Bronze Component in Nb_3Sn Conductors Through Ultimate Strength Measurements

Dixon, I.R., NHMFL
Markiewicz, W.D., NHMFL

The bronze matrix in the Nb_3Sn conductors for the wide bore 900 MHz NMR magnet is the least ductile component. An excessively brittle bronze matrix could lead to fracture during the process of bending the conductor. To quantify this, room temperature ultimate strength measurements are performed. Ultimate strength and strain of the five wire types are reported.

A representative sample from each conductor type was made. Copper support tabs were used between the samples and grips. A tapered geometry of the tab was made to improve the stress flow to the test section. Each sample is nominally 150 mm (6") long with a 50.8 mm (2") gage length between support tabs. The geometry of each conductor type is given in Table 1.

Table 1. Geometric configuration of Nb_3Sn samples for 900 MHz magnet.

Coil	h (mm)	w (mm)	R (mm)	A_w (mm^2)
1	1.970	3.150	0.300	6.128
2	1.680	2.860	0.300	4.728
3	1.390	2.370	0.300	3.217
4	1.180	1.960	0.300	2.236
5	1.000	1.690	0.300	1.613

Table 2. Ultimate tensile test results at room temperature.

Coil #	1	2	3	4	5
l_0	50.80	50.80	50.80	50.80	50.80
σ_p	20.0	20.0	20.0	20.0	20.0
u_i	0.0427	0.8782	0.0471	0.1348	0.0081
u_{max}	3.35	4.78	2.72	3.89	2.43
Δu	3.31	3.91	2.67	3.76	2.42
ε_u	6.51	7.69	5.25	7.39	4.76
σ_u	597.6	675.8	729.8	650.4	609.0

The tests were performed without any external strain measurement devices. The load and crosshead strokes were recorded. The strain associated with the relative displacement is computed by taking into account the stiffness of the test machine, measured to be approximately 12523 N/mm.

In computing the strain, a prescribed stress is given to come up with an initial offset displacement (u_I). This is used to shift the data to get it away from the tail that develops while the sample straightens. The total deformation is then computed by $\Delta u = u_{max} - u_i$. The ultimate strain is then determined through $\varepsilon_u = \Delta u / l_o$. The ultimate strain and stress for each sample is given in Table 2 for each coil. Figure 1 contains the stress-displacement curves for each conductor type.

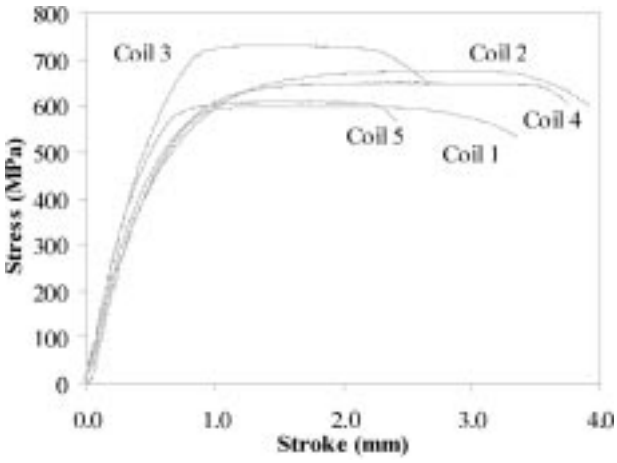

Figure 1. Ultimate strength measurements of Nb_3Sn wires at room temperature.

The most brittle conductors are shown to be from coils 3 and 5. Coil 1 is moderately brittle with a strain to failure of 6.5%. Conductors for coils 2 and 4 have the highest strengths of greater than 7%.

Computation of the Magnetic Loads Applied by the Superconducting Joint Correction Coils of the 900 MHz NMR Magnet

Dixon, I.R., NHMFL
Markiewicz, W.D., NHMFL

A concept of free-supported leads is employed in the 900 MHz NMR magnet design. The concept incorporates a structural tower that supports the superconducting leads and splice joints, but does not constrain the axial motion. The lead support towers guide the leads to a plate where joints are made. Each joint is inserted into a bucking coil to reduce the local magnetic field. The bucking coils are mounted on steel support arms that attach to the top of the lead support towers. The base of the support towers is rigidly bolted to the top of the coil forms. Splice leads have zero net force, but the end leads distribute a nonlinear load along the height of the towers. The bucking coils apply a torque, radial force, and axial force to the ends of the tower, at the support arms. The lead loads for each coil of the 900 MHz magnet have been computed for a stress analysis of the towers. The formulation of the loads is discussed here.

The loads on the lead towers come from the interaction between the leads, bucking coils, and the main magnet. A differential transverse force is exerted on the superconducting lead because of the radial field, and is expressed as

$$\frac{dF}{dl} = \vec{I} x \vec{B} \qquad (1)$$

This may be solved piecewise by examining the field in the neighborhood of the lead. The superconducting leads place a distributed load along the tower sidebars, and may be represented over a range by a polynomial, up to order $n = 6$, in the form

$$w(z) = \sum_{i=1}^{n} a_i z^i \qquad (2)$$

This may be integrated to obtain the total force (F_D) applied on the structure. Division by the load application length gives an average distributed force. The resultant superconducting lead load is the total force applied at the centroid of the distribution curve, which is given by

$$\bar{z} = \frac{\int z\, w(z)\, dz}{\int w(z)\, dz} \qquad (3)$$

Forces and torques exist on the bucking coil because of the interaction with the external field of the main magnet. The forces are given by

$$\vec{F} = (\vec{m} \cdot \nabla)\vec{B} \qquad (4)$$

where $\vec{m}$ is the dipole moment of the bucking coil. The dipole moment of all bucking coils is assumed to be the same, and is oriented in the axial direction. The dipole moment of the bucking coil is

$$\vec{m} = NIA\hat{j} = -31.19\hat{j} \qquad (5)$$

where $\hat{i}, \hat{j}, k$ are unit vectors oriented in the r, z, θ directions, respectively. The radial and axial force components that result from the dot product are

$$F_R = m_z \frac{\partial B_R}{\partial z} \qquad (6)$$

and

$$F_z = m_z \frac{\partial B_z}{\partial z} \qquad (7)$$

The torque is the cross product between the dipole moment and magnetic field, expressed as

$$\vec{\tau} = \vec{m} \times \vec{B} \qquad (8)$$

Only a tangential component of the torque exists since the axial field component is directed in the same direction as the dipole moment. From the radial field component the torque becomes

$$\vec{\tau} = mB_R\hat{k} \qquad (9)$$

The torque is applied to the support arms through the bucking coil end flanges, which are a nominal 72.7 mm apart from each other. Thus the torque is resolved into two radial forces which are applied to the arms. At the uppermost point the torque force is applied in the negative direction, and at the lower point the torque force is applied in the positive direction. To compute the loads, the magnetic field is approximated by a polynomial for each coil.

Critical Current of Nb_3Sn Conductors for the Wide Bore 900 MHz NMR Magnet

Dixon, I.R., NHMFL
Markiewicz, W.D., NHMFL
Pickard, K.W., NHMFL
Swenson, C.A., NHMFL

A wide bore, high resolution NMR magnet is currently under construction at the NHMFL. The magnet will be capable of a spectrometer frequency of 900 MHz and a field of 21.1 T with operation at 1.8 K. The magnet consists of epoxy impregnated, high current density Nb_3Sn, and NbTi coils with lumped external reinforcement where required.

The magnet brings forth many technological challenges that require efficient use of available materials. To achieve this, a detailed knowledge of their physical properties is needed. The focus here is to present the electrical characterization of the superconductors for the Nb_3Sn coils. Electrical measurements at 4.2 K and 1.8 K have been conducted in steady state background fields up to 19.45 T. A sample from each coil piece length was prepared by a wind and react method. The samples were then attached to one of two sample holders across a Ti-6Al-4V shunt via a solder dip method. The critical currents of each sample through a range of fields are recorded.

The construction of the superconductors is unique for each coil in dimensions and number of filaments. The superconductor designations, component fractions, and filament quantity are listed in Table 1.

Table 1. Nb_3Sn superconductor component configuration.

Type	Coil	f_{Cu}	f_{SC}	$f_{Barrier}$
NSTT 86000A25	1	0.25	0.69	0.06
NSTT 62000A25	2	0.25	0.69	0.06
NSTT 64000A25	3	0.25	0.69	0.06
NSTT 62000A25	3	0.25	0.69	0.06
NST 39000A33	4	0.34	0.61	0.05
NST 28000A49	5	0.49	0.46	0.05

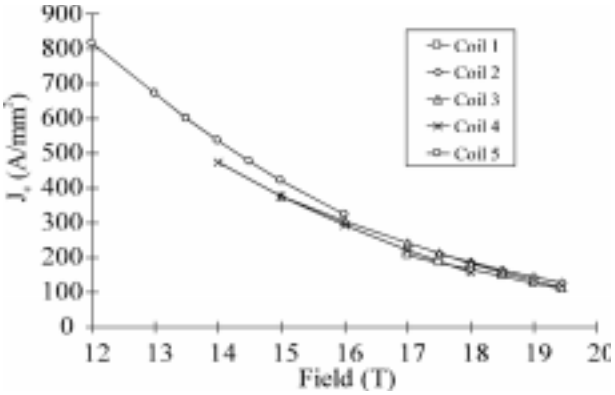

Figure 1. Critical current density of conductors from each coil of the 900 MHz NMR magnet as a function of field and at a temperature of 4.2 K.

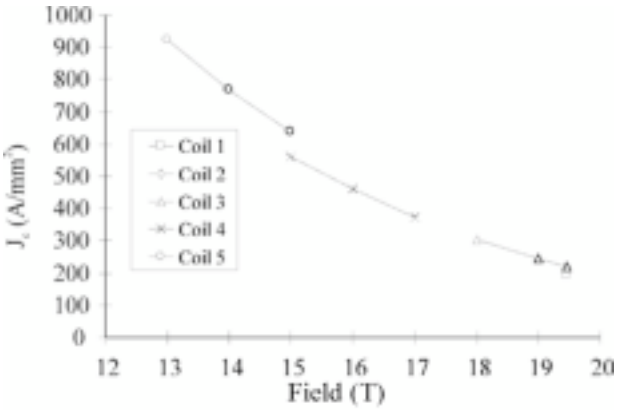

Figure 2. Critical current density of conductors from each coil of the 900 MHz NMR magnet as a function of field and at a temperature of 1.8 K.

The superconducting transition is defined when the differential voltage above the baseline voltage is 0.1 μV/cm of sample length. The baseline voltage is the averaged initial voltage of the sample during the current ramp prior to transitioning to normal. The sample length is measured along the path of the neutral axis of the conductor, and is nominally 28 mm. The critical current density as a function of field for a conductor sample of each coil is plotted in Figure 1 at a temperature of 4.2 K, and in Figure 2 at a temperature of 1.8 K. The measured and computed results meet the specifications for the magnet and exceed the expected values used in the magnetic design.

Magnetic Characterization of Steel and Weld Alloys for NMR Coil Forms

Swenson, C.A., NHMFL
Markiewicz, W.D., NHMFL

Magnetic field uniformity is critical to NMR. Historically, magnet designs have avoided ferrous alloys to prevent field distortions by the structure. Zhukovsky, *et al.*, choose, in the MIT 750 MHz, to avoid the non-magnetic 316 series stainless steels.[1] This philosophy presents a serious challenge to the magnet designer because austenitic stainless steel is the preferred heat treatment material for bore tubes in Nb_3Sn coils. Removal of the bore tube after heat treatment and epoxy impregnation is unacceptably dangerous due to the risk of damaging the Nb_3Sn. A more practical approach is to leave the stainless steel bore tubes in place. The magnetic contribution, from the permeability of the coil forms, is symmetrical, and can be calculated and corrected for the design of the shims. The critical issue is the magnetic properties of the weld metal. The welds, particularly in a seemed tube, are not symmetrical. Our objective is to control the permeability in the weld metal. This can be accomplished by producing zero ferrite welds.

We identified three weld metal alloys for joining 316L:SS with zero ferrite welds. Two alloys, Grinox T-51 and the LNT/LNM 4500, are commercially available from Lincoln Electric. The third alloy is a BNL-NIST super-alloy developed for the RHIC program.

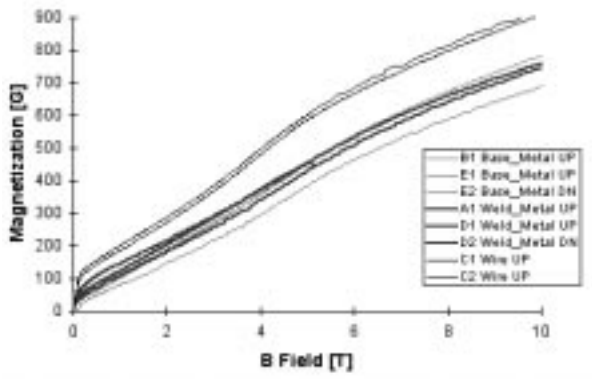

Figure 1. Magnetization of 316:SS and weld metal.

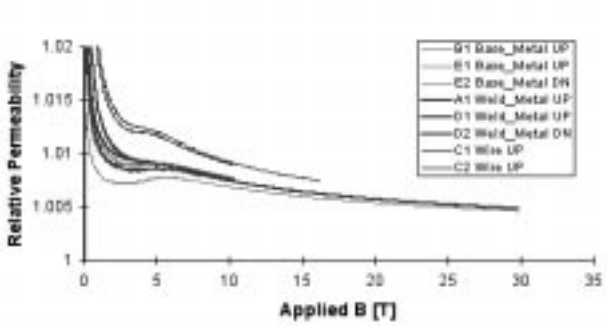

Figure 2. Permeability of 316:SS and weld metal.

The Grinox T-51 weld alloy was used to join three steel weld coupons. The stainless steel complied to DIN 17441-composition 1.4404. Our evaluation included a measurement of ferrite number using a magnigage at NIST, and a 4 K measurement of the magnetization using a vibrating sample magnetometer at NHMFL.

The measured ferrite number was zero in the base metal, weld region, and the near heat zone around the welds. Figure 1 presents the magnetization measurements for base metal and weld samples. There is at most a 50 gauss saturation offset in the curves for the weld samples. Figure 2 plots the relative permeability of the samples. The permeability of the weld and base metal is <1.01 at fields above 5 T.

The Grinox weld alloy performed acceptably. There is a general consensus that either of the other weld alloys would also be satisfactory for NMR applications. The weld permeability can be controlled with sufficient attention to the weld alloy and the base metal.

Reference:

1 Zhukovsky, A., *et al.*, IEEE Trans. Magn., 28, 1 (1992).

Magnetic Characterization of Steel Reinforcement Alloy for NMR Applications

Swenson, C.A., NHMFL
Dixon, I.R., NHMFL
Markiewicz, W.D., NHMFL

High field magnets require reinforcement to contain the electromagnetic stress. The 900 MHz design employs a rectangular copper clad 316L steel reinforcement wire. There are several layers of reinforcement on the outside of the stressed coils in the design.

Magnetic field uniformity is critical to NMR. Our objective is to control the permeability of the reinforcement steel. The critical issue is the magnetic permeability of the reinforcement under cyclic stress. The 316L:SS can work harden during cryogenic cycling. The steel may undergo a phase transformation to martensite during this work hardening. The magnetic properties of the material would be undesirable if such a phase transformation occurs. Twelve samples of over-banding were tested at 4.2 K using a vibrating sample magnetometer measurement technique. The samples were prepared from tensile test wires that were strain cycled at 4.2 K to simulate the strain environment of an energized magnet. The maximum design strain of the 900 MHz reinforcement is approximately 0.25%. Table 1 provides an outline of the sample preparation.

Table 1. Summary of sample preparation.

Samples	Cycles	Strain
A1 & A2	1	0.25%
B1 & B2	10	0.25%
C1& C2	50	0.25%
D1 & D2	100	0.25%
E1 & E2	10	0.30%
F1 & F2	1	3.40%

The VSM samples were machined from the wire samples after tensile cycling. The martensite resulting from work hardening is stable since the reversion temperatures of the martensite phases are 410 °C for the ε phase, and 770 °C for the α′ phase.[1] Figure 1 presents the VSM measurements for the wire samples. Figure 2 plots the relative permeability of the samples.

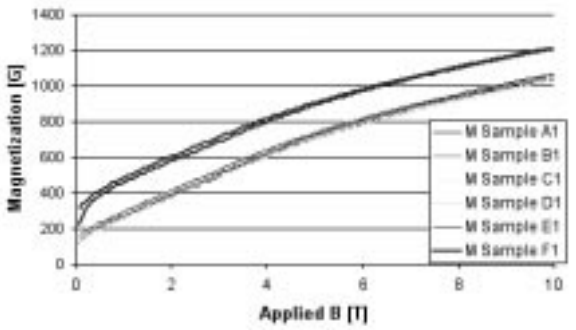

Figure 1. Magnetization of reinforcement wire.

The permeability of the 316L reinforcement wire did not exhibit cyclic strain dependence below 0.30%. The permeability is less than 1.015 at fields above 5 T. Sample F1 & F2 showed a 100 G offset with a strain of 3.4%. The work hardening of 316L:SS does not appear to be an issue with proper selection of alloy chemistry.

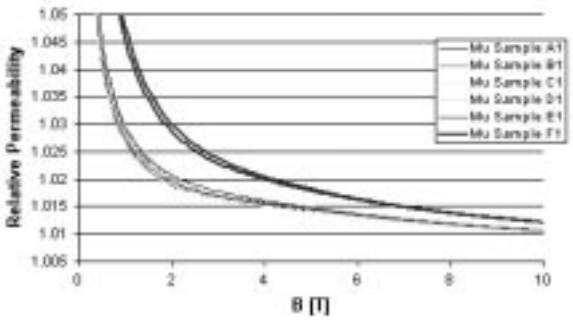

Figure 2. Permeability of 316L:SS and weld metal.

Reference:

1 Reed, R.P., Materials at Low Temperatures, Chapter 9, pub. ASM 1983.

Testing of a 2.5 T Class HTS Insert Coil

Weijers, H.W., NHMFL
Viouchkov, Y., NHMFL
Van Sciver, S.W., NHMFL/FAMU-FSU College of Engineering
Hazelton, D., Intermagnetics General Corp.

The testing of a 2.5 T Class Insert Coil was the final task of a Phase II SBIR project with Intermagnetics General Corp. (IGC) with the goal of developing magnet technology for high field NMR insert coils based on high temperature superconductors (HTS). The insert coil was built by IGC, with a design based on the results of collaborative research. The 2.5 T Class Insert Coil was built using layer winding react and wind (R&W) techniques with surface coated Bi-2212 tape and glass fiber in the windings, overbanded with stainless steel. It has 3 concentric sections, a clear bore of 52 mm, and an overall outer diameter of 160 mm. With a winding height of 0.2 m and 2.3 km of conductor, it is a sizeable HTS coil. It was tested in the 20 T large bore resistive magnet at the NHMFL, using an insert cryostat with a 170 mm cold bore.

Apparently, section 1 (inner section) sustained some unexpected degradation somewhere in the process of fabrication, transport or cool down, as it limited the performance at a critical current (I_c) level below expectation. The I_cs of sections 2 and 3 were higher than the quench current for section 1, and could, therefore, not be determined. The coil was tested to 19 T in the second run. The first run was terminated after 5 T, when the power supply of the resistive magnet tripped. That trip changed the magnetization, and therefore I_c at 0 T, but not the I_c at 5 T, from which it is concluded that no damage was done. Figures 1 and 2 show test results. The 2.5 T Class Insert Coil generated 2.5 T at self-field and 1.5 T in a 19 T background. That value can be increased significantly by powering sections 2 and 3 separately, or replacing section 1.

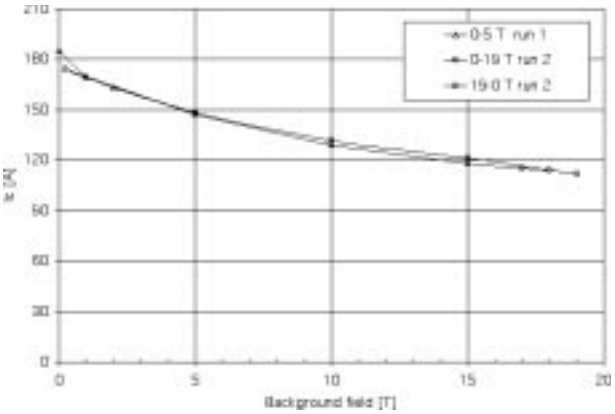

Figure 1. Critical current vs. applied magnetic field relation for section 1.

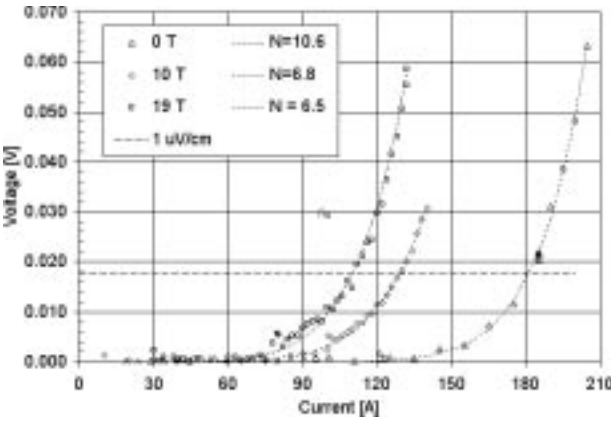

Figure 2. Voltage-current curves for section 1 in a background of 0, 10, and 19 T. The lines through the data points are power law fits with the N-values listed in the legend.

Summary: A 2.5 T Class Bi-2212/Ag Insert Magnet constructed by IGC was tested at 4.2 K, generating 2.5 T at self-field and 1.5 T in a 19 T background. This technique is viable and has the potential to generate higher fields.